Fourier transform mid- and far-infrared specular reflectance studies of the polarizability of ion-containing polymers and oxidized polyethylene and its application to adhesion

Hans-Peter Brack*† and William M. Risen, Jr.

Department of Chemistry, Brown University, Providence, RI 02912, USA

The dielectric properties of selected ion-containing polymers have been studied by specular reflectance spectroscopy through the mid- and far-infrared regions. These reflectance spectra and the resulting dielectric spectra were measured on (1) surface-oxidized and cation-exchanged polyethylene and bulk ionomers based on (2) ethylene-*co*-methacrylic acid copolymers, and (3) partially *para*-sulfonated polystyrene. The chemical nature of the near surface region and its response to applied fields was studied for these materials. The far-infrared spectra were studied to examine the interaction of metal cations with anionic sites, and the polarizability in the far-infrared was found to vary systematically with the identity of the cation. Adhesion forces resulting from dispersion interactions due to polarization mechanisms at mid- and far-infrared frequencies were calculated by Lifshitz theory for polymer–Pyrex glass substrate pairs.

It is widely recognized that covalent, ionic, and hydrogen-bonding, acid–base (or donor–acceptor) interactions, dispersion (polarization) interactions, and, to a lesser extent, electrostatic interactions can contribute to adhesion.[1] However, little quantitative information or consensus exists as to the importance of particular forces or mechanisms for adhesion except in certain specific systems.

In the present work, the polarization at frequencies corresponding to the mid- and far-infrared spectroscopic regions of polymers containing ionic functional groups has been measured. Such materials have strong absorption bands in these regions, so it is possible to measure these polarization properties. The contributions of surface-oxidized groups to dispersion at these frequencies and to adhesion interactions have been evaluated from dielectric properties that were determined from measured normal incidence specular reflectance (NISR) spectra. The NISR spectra of oxidized polyethylene surfaces and the NISR spectra of ionomers have been studied. The systems studied include (1) polyethylene that has been 'surface-oxidized' with chromic acid, in a process that introduces carboxylic acid groups, and the same materials after ion exchange of the acidic protons by various alkali metal cations. These are labelled PE(ox-H^+) and PE(ox-M^+), respectively. They also include bulk ionomers and their acid precursors, such as (2) ethylene-*co*-methacrylic acid copolymers (EMAA-M^+ and EMAA-H^+), (3) ethylene-*co*-acrylic acid copolymers (EAA-H^+), and (4) partially *para*-sulfonated polystyrene (SPS-M^+ and SPS-H^+).

The bulk ionomers are useful analogs to PE(ox-H^+) and PE(ox-M^+) for this application of the relatively little used NISR technique. They exhibit 'ion-motion bands' in the far-infrared, which are due to cation-site vibrations. Such bands were first observed for alkali ions in solution by Risen and co-workers[2] and later by Maxey and Popov.[3] Ion-motion bands were later also found in the far-infrared spectra of ionomers,[4–8] glasses,[9] alkali ion salts dissolved in solution of crown ethers[10] or polyethers,[11] and zeolites.[12] These bands are strong because of the large dipole moment changes associated with the periodic cation–anionic site displacements, and they are cation–specific due to the strong cation mass dependence of the resonant frequencies. Moreover, the spectral changes in this region, specifically the shifts of the ion-motion band that occur when the cation is changed, are well understood from our previous work.[2,4,5–10,12] The ethylene-*co*-methacrylic acid and ethylene-*co*-acrylic acid copolymers provide for a spectroscopic comparison to the surface-oxidized PE(ox) system, and the ionomers have some of the types of chemical features that might be found on cation-exchanged PE(ox) surfaces, so they can help to locate and identify them.

The present investigation examines specifically the influence of cation exchange, cation identity and ion content on the surface polarizability of these materials. In this work, the far-infrared as well as the mid-infrared range values of the dielectric functions have been obtained by NISR spectroscopy. They have then been used to calculate dispersion forces and Hamaker constants.[13–15]

Although polarization mechanisms at all frequencies can contribute[13] in principle to dispersion interactions between macrobodies, Gingell and Parsegian[14] were among the first to propose that dipole moment changes and polarization changes in the infrared frequency region could be important in adhesion interactions. Their calculations in their study on the contributions of various frequency regions to the interaction energy for water across a lipid film indicated that a substantial contribution comes from the infrared region. Belyi, Smurugov and Sviridyonok[15] have suggested that dispersion interactions, and especially the contribution to them from the mid-infrared region, contribute to the greater strengths of joints formed with surface-oxidized polyethylene, PE(ox), than with untreated PE. In addition, they measured the imaginary part of the dielectric function in the mid-infrared region for a series of polar and non-polar polymers and found that while the infrared region makes only a small contribution to the static relative permittivity for relatively non-polar polymers, such as PE and PP, its contribution is considerably larger for more polar polymers.

The contributions of various polarization mechanisms and thus frequency ranges to the static relative permittivity can be important in dispersion interactions. For example, Prieve and Russel[16] found that the static relative permittivity is an important term in determining the dispersion interaction for the polystyrene/H_2O/polystyrene system. In fact, some approximate solutions for the calculation of dispersion forces in special cases use only the value of the static relative permittivity for

* E-mail: hanspeter.brack@psi.ch
† Present address: Elektrochemie, Paul Scherrer Institut, CH-5232 Villigen, Switzerland.

the materials.[17] Rabinovich and Churaev[18] demonstrated that adhesion treatments which ignore the infrared and lower frequency regions were applicable for only those materials having very weak absorbance in the infrared, and that even in that case it is necessary to add a zeroth-order term for the static relative permittivity. Thus, polarization mechanisms at infrared frequencies exert an influence on dispersive adhesion forces since they also contribute to the static relative permittivity for these materials.

Of relevance to the present study are the experimental adhesion studies of Lipatov and co-workers,[19] who investigated the adhesion of ionomeric interpenetrating polymer network (IPN) materials to various glass and metallic substrates. They found that the adhesion increased with increasing concentration of ionic groups, and that it increased for the same concentration of ionic groups but differing cations in the order: $K^+(^-OOCR) < Na^+(^-OOCR) < Li^+$ (^-OOCR). The observed changes in adhesion were not attributed directly to dispersion forces nor were any dispersion forces calculated, but their study provides adhesion data that are useful to compare to the dispersion forces calculated from the spectral data obtained in this work. Additional studies of adhesion of ionomers and their acid copolymers to rubber composites,[20] as well as reviews of the use of sulfonic acid[21]- and carboxylic acid[22]-containing ionomers as adhesives have been published.

Experimental

Materials

Polyethylene and oxidized polyethylene [PE(ox)] and its exchange. The preparation of optically thick oxidized, and, in some cases, ion-exchanged, low density polyethylene, PE(ox) and PE(ox-M^+), respectively, was carried out using our reported methods[23] using low density PE in slab form obtained from Franklin Fibre-Laminex Corp. Briefly, the samples were smoothed by heating at a PTFE (*e.g.* Teflon)-covered surface before oxidation with chromic acid and subsequent ion-exchange. The PE(ox) samples were ion-exchanged to replace the H^+ of the PE(ox-H^+) to prepare the PE(ox-M^+) forms by reacting them with the metal methoxide in methanol under nitrogen atmosphere for 1 h, and washing them with methanol.

Ethylene-*co*-methacrylic acid and ethylene-*co*-acrylic acid copolymers. The un-ionized acid form of the ethylene/methacrylic acid (EMAA) copolymer and the ion exchanged forms were kindly prepared and supplied by the Du Pont Company. The average molecular mass of the EMAA copolymer is 3.0×10^5 g mol^{-1}. The hydrogen, lithium, sodium and caesium forms of the 7.6 mass% methacrylic acid (2.6 mol%) and the hydrogen and potassium forms of the 15 mass% methacrylic acid (5.4 mol%) EMAA copolymer were studied. Slabs suitable for specular reflectance analysis were prepared by fusing together several pieces of material between PTFE sheets in a vacuum oven at 145 °C for 15 min.

Samples of the acid (un-ionized) form of ethylene/acrylic acid (EAA) copolymers, Dow Primacor 3150 (1.2 mol% acrylic acid), Primacor 3340 (2.7 mol% acrylic acid), and Primacor 3460 (3.9 mol% acid), were obtained in pellet form. Optically thick slabs of these un-ionized EMAA and EAA copolymers were prepared by melting several grams of the bead form of the copolymer onto a PTFE substrate in vacuum at 145 °C under several psi pressure.

Sulfonated polystyrene. Acid-form *para*-sulfonated linear polystyrene (SPS-H^+) material was provided by Dr Robert Lundberg of the Exxon Chemical Company. The SPS material used in this study had 12.8% of the rings sulfonated. The SPS-M^+ ionomers were prepared by reaction in tetrahydrofuran (THF)–H_2O solution with the alkali metal nitrate salt containing the desired cation. The exchanged material was thoroughly washed with deionized water, dissolved and precipitated several times. Samples in the form of approximately 7 mm thick slabs on top of glass plate substrates were prepared by repeated casting and drying of the metal-SPS samples dissolved in 10 : 90 (v/v) water–tetrahydrofuran solution. The solvent in the formed slabs was evaporated on a vacuum line prior to spectral analysis.

Spectral methods

The reflectance FTIR measurements were made on an IBM/Bruker IR98 with an evacuated 113v optics bench. Far-infrared spectra were obtained with an Infrared Laboratories Model HD-3 doped silicon bolometer operating at liquid helium temperature. All samples were dried on a vacuum line for 12 h and then transferred rapidly to the sample chamber of the FTIR spectrometer, where they were kept under vacuum for an additional 90 min prior to spectral analysis. All reflectance spectra were measured over the 10–4500 cm^{-1} range using a specular reflectance accessory with a near normal angle of incidence of 87° and were calculated from the sample power spectra by calculating their ratio to the power spectrum of a Au–Cr plated flat mirror.

The reflectance spectrum for each sample in the 20–4000 cm^{-1} was transformed then into the complex refractive index $[n^*(\omega) = n(\omega) + ik(\omega)]$ and dielectric function $[\varepsilon^*(\omega) = \varepsilon'(\omega) + i\varepsilon''(\omega)]$ using our previously reported methods.[24] Briefly, the phase change upon reflectance, $\phi(\omega)$, was determined by a Kramers–Kronig transformation (KKT) of the reflectance spectrum, R. The complex refractive index was next determined from $R(\omega)$ and $\phi(\omega)$ using the Fresnel equation, and then ε^* was calculated from n* $[\varepsilon^*(\omega) = |n^*(\omega)|^2]$. The dielectric functions $\varepsilon'(\omega)$ and $\varepsilon''(\omega)$ are measures of the polarizability and absorbance, respectively.

Results

Reflectance spectra

The reflectance spectra of the materials described above were measured on optically thick samples to ensure the validity of the KKT-based determination of the dielectric functions. This required that (1) the samples should have very low (*ca.* zero) transmittance, (2) there should be no interference fringes in their reflectance spectra and (3) there should be no interference signature peaks in their interferograms. The NISR-measured spectra of the near surface regions of oxidized and subsequently ion-exchanged PE(ox-M^+) are broad and weak. Observing them required many scans, so it is important to identify them with certainty. The advantage of studying several related materials with different cations is seen here. The spectral changes that occur when the materials were exchanged with different cations or when a material was re-exchanged with a new cation made it possible to confirm that the observed spectral variations occurred on bands whose frequencies vary as a function of cation identity.

Mid-infrared spectra

The NISR-measured mid-infrared spectrum of chromic acid-oxidized low density polyethylene, PE(ox), showed bands in the 1700–1750 cm^{-1} region due at least to hydrogen bonded and isolated carboxylic acid (1710 and 1750 cm^{-1}, respectively), ketone (1721 cm^{-1}) and aldehyde (1733 cm^{-1}) functional groups. The peak absorbance of the carboxylic band at 1710 cm^{-1} decreases and a band due to the asymmetric CO_2^- stretching mode appears at 1550 cm^{-1} when the PE(ox), *i.e.* PE(ox-H^+), is treated in alkali methoxide solution to exchange M^+ for H^+. No bands for carbonate ion or methoxide bands

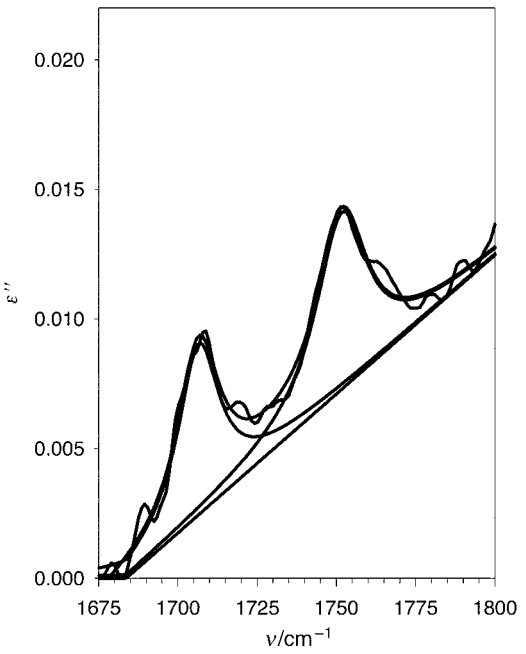

Fig. 1 Mid-infrared ε'' spectrum resulting from the spectral subtraction of the spectrum of the H^+ form of PE(ox) minus that of PE(ox-Na^+). The fitted bands and baseline are shown also.

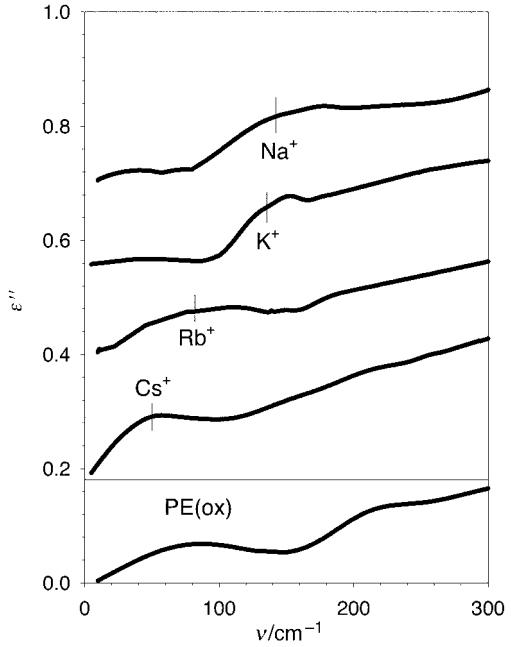

Fig. 2 Far-infrared ε'' spectra of PE(ox) and PE(ox-M^+) ($M^+ = Cs^+$, Rb^+, K^+ and Na^+). The spectra of the cation-exchanged forms include an arbitrary offset.

appeared upon exchange, and no bands were observed to indicate ester formation.

Spectral subtraction was used to obtain information on the nature of the carboxylic acid groups that were exchanged in the treatment with alkali methoxide solutions. For example, subtraction of the spectrum of the mid-infrared spectrum of PE(ox-Na^+) from that of the unexchanged H^+ form of the sample, shown in Fig. 1, yields the absorption bands of the H^+ form which are not present for the Na^+ form of PE(ox). Two absorption features, one at 1750 cm^{-1} (monomers) and the other at 1710 cm^{-1} (dimer form), are observed for carboxylic acid and disappear or diminish when H^+ is replaced by Na^+ or another cation. This region was fitted with Lorentzian bands and a sloping baseline to find that the ratio of the integrated absorbance of the 1710 to the 1750 cm^{-1} band varied between 0.65 : 1.0 to 0.80 : 1.0 for the subtraction spectra. Using the relationship between the magnitudes of the integrated absorbances for carboxylic acid dimers and monomers in EMAA copolymers reported by MacKnight and co-workers,[25] the carboxylic acid groups of PE(ox) that were exchanged in this investigation are calculated to be about 55–60% in the monomer form and 45–40% in the dimer form.

Spectral integration in the carbonyl region of the MIR spectra of the EMAA ionomers indicated that typically 60% of the carboxylic acid groups are exchanged. No bands for carbonate or nitrate ions appeared upon exchange of the SPS-H^+.

Far-infrared spectra

Far-infrared spectra of the near surface region of the PE(ox) and PE(ox-M^+) ($M = Cs^+$, Rb^+, K^+ and Na^+) materials are shown in Fig. 2 for the ε'' spectra and in Fig. 3 for the ε' spectra. Broad, weak far-infrared bands are observed for the PE(ox-M^+) samples. The effective concentration of the carbonyl functionalities is low because the spectral penetration depth into PE(ox) is greater than the depth of functionalization due to oxidation. Fortunately the behavior of alkali carboxylate-containing ionomers in this region is well understood from our previous work,[4–8] so it is clear that the far IR bands observed at 400 cm^{-1} for the Li^+ form, 150 cm^{-1} for the Na^+ form, 135 cm^{-1} for the K^+ form, 90 cm^{-1} for the

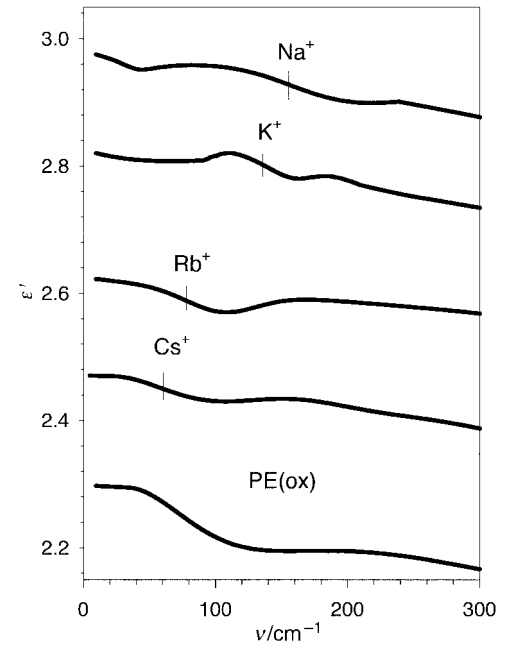

Fig. 3 Far-infrared ε' spectra of the PE(ox) and PE(ox-M^+) ($M^+ = Cs^+$, Rb^+, K^+ and Na^+). The spectra of the cation-exchanged forms include an arbitrary offset.

Rb^+ form and 55 cm^{-1} for the Cs^+ form are due to ion-motion bands.[2–12]

When a PE(ox-M^+) sample is re-exchanged with another cation, the cation-motion band for the first cation disappears and that due to the second cation appears. For example, the PE(ox-Na^+) sample whose spectrum is shown in Fig. 2 is that of a PE(ox-K^+) sample re-exchanged with Na^+. These far-infrared ion-motion bands disappeared when the sample surface was treated with a weak acid solution. The polarizability of a PE(ox-M^+) sample increases as the ion-motion band is approached from the high frequency side. In the case of unionized PE(ox-H^+) the increase begins at about 100 cm^{-1}. The magnitude of this increase in polarizability varies as PE(ox-H^+) > PE(ox-Li^+) > PE(ox-Na^+) > PE(ox-K^+) > PE

(ox-Rb^+) > PE(ox-Cs^+). The $\Delta\varepsilon'$ values for the far-infrared region are shown in Table 2.

The far-infrared ε'' spectra of the H^+, Li^+, Na^+ and Cs^+ forms of the 2.6 mol% acid EMAA copolymers, (EMAA-H^+, EMAA-Li^+, EMAA-Na^+, and EMAA-Cs^+), are shown in Fig. 4. Also shown, but reduced to half scale for comparison purposes, is the spectrum of the K^+ form of the 5.4 mol% acid EMAA copolymer. The frequencies of the ion-motion bands are shown in Table 1, as well as the ion-motion band frequencies of analogous EMAA copolymers determined[5–6] previously from transmission measurements.

The far-infrared ε' spectra for these samples are in Fig. 5. An increase in the polarizability of the material occurs as the frequency of the ion-motion band in EMAA ionomers (or about 75 cm^{-1} in the un-ionized EMAA) is approached from the high frequency side. The magnitude of this increase in polarizability varies for the exchanged forms of 2.6 mol% acid EMAA copolymer as (EMAA-H^+)>(EMAA-Li^+)>(EMAA-Na^+)>(EMAA-Cs^+). This trend is shown in Table 2, in which both the mid- and far-infrared regions are considered together. The $\Delta\varepsilon'$ values for the 5.4 mol% EMAA copolymers indicate that the increase in polarizability is considerably larger in the higher acid and higher ion content materials.

The ε'' and the ε' spectra for hydrogen-form EAA samples show, as in the case of the 2.6 and 5.4 mol% hydrogen-form EMAA, a broad band envelope in the 200–450 cm^{-1} region of the ε'' spectra. This feature increases in strength as the acid content increases. The ε' spectra show a gradual increase in polarizability with decreasing frequency starting at about 600 cm^{-1} and which becomes quite steep at about 75 cm^{-1}, as in the EMAA copolymers. This increase in infrared polarizability with increasing acid content is also tabulated in Table 2.

The ε'' and the ε' spectra of the SPS ionomers are shown in Fig. 6 and 7, respectively. The ion-motion band frequencies are listed in Table 1, and the increases in polarizability in the infrared region observed for the ε' spectra are tabulated in Table 2. Similar to the results for the EMAA ionomers the increase in polarizability ($\Delta\varepsilon'$) in the far-infrared region for SPS is in the order: SPS-Li^+ > SPS-Na^+ > SPS-K^+ > SPS-Rb^+ > SPS-Cs^+. The increase in ε' for the H^+ form of SPS is less than that of the exchanged alkali cation forms but greater than that of PS.

Table 1 Ion-motion band frequencies

polymer	acid content (mol%)	cation identity	ion-motion band frequency, ν/cm^{-1} specular reflectance (ε'')	ion-motion band frequency, ν/cm^{-1} transmission (%T)
PE(ox)	—	Li^+	400.±10.	N.D.[a]
PE(ox)	—	Na^+	150.±10.	N.D.
PE(ox)	—	K^+	135.±10.	N.D.
PE(ox)	—	Rb^+	90.±10.	N.D.
PE(ox)	—	Cs^+	55.±10.	N.D.
EMAA	2.6	Li^+	415.±7.	450±5[b]
EMAA	2.6	Na^+	200.±7.	230±5[b]
EMAA	5.4	K^+	175.±7.	180±5[b]
EMAA	2.6	Cs^+	95.+7.	135±5[b]
SPS	12.8	Li^+	430.±7.	N.D.
SPS	12.8	Na^+	175.±7.	210±5[c]
SPS	12.8	K^+	135.±7.	160±5[c]
SPS	12.8	Rb^+	110.±7.	120±5[c]
SPS	12.8	Cs^+	85.±7.	100±5[c]

[a]N.D.: Not determined. [b]Ref. 5 and 6. [c]Ref. 4 and 7.

Table 2 $\Delta\varepsilon'$ in infrared region

polymer	acid content (mol%)	cation identity	$\varepsilon'(\nu_1)$[a]	$\varepsilon'(\nu_2)$[a]	$\Delta\varepsilon'$
PE(ox)	—	H^+ (un-ionized)	2.28	1.96	0.32
PE(ox)	—	Li^+	2.22	1.97	0.25
PE(ox)	—	Na^+	2.20	1.97	0.23
PE(ox)	—	K^+	2.18	1.99	0.19
PE(ox)	—	Rb^+	2.16	2.01	0.15
PE(ox)	—	Cs^+	2.11	1.96	0.15
EMAA	2.6	H^+ (un-ionized)	3.25	1.73	1.52
EMAA	2.6	Li^+	2.84	1.75	1.09
EMAA	2.6	Na^+	2.52	1.73	0.79
EMAA	2.6	Cs^+	2.37	1.76	0.61
EMAA	5.4	H^+ (un-ionized)	3.93	1.78	2.15
EMAA	5.4	K^+	2.60	1.74	0.86
EAA	1.2	H^+ (un-ionized)	2.43	1.61	0.82
EAA	2.7	H^+ (un-ionized)	2.63	1.65	0.98
EAA	3.9	H^+ (un-ionized)	2.68	1.63	1.05
PS	—	—	2.56	2.33	0.23
SPS	12.8	H^+ (un-ionized)	2.94	2.64	0.30
SPS	12.8	Li^+	3.99	2.66	1.33
SPS	12.8	Na^+	3.72	2.69	1.03
SPS	12.8	K^+	3.50	2.71	0.79
SPS	12.8	Rb^+	3.43	2.70	0.73
SPS	12.8	Cs^+	3.23	2.68	0.55

[a]$\varepsilon'(\nu_1)=20$ cm^{-1} for all cases. $\varepsilon'(\nu_2)=3500$ cm^{-1} for all cases except PE(ox), where it is equal to 650 cm^{-1}.

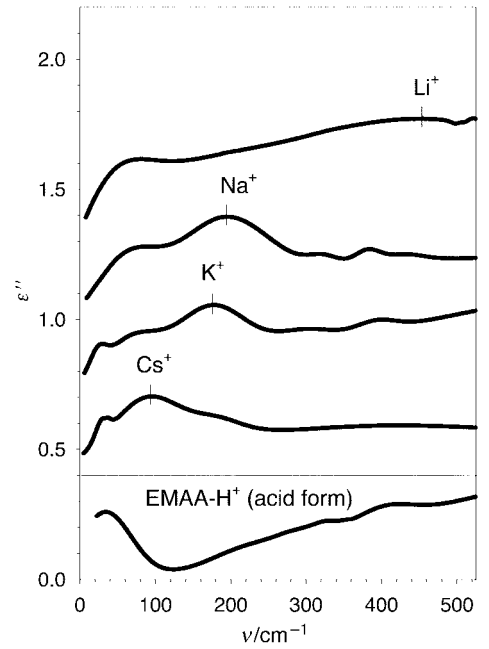

Fig. 4 Far-infrared ε'' spectra of the H^+ (acid), Cs^+, K^+, Na^+ and Li^+ forms of the EMAA copolymers. The K^+ form is that of the 5.4 mol% acid material and is shown 50% reduced in scale for ease of comparison with the other spectra, all of which are of the 2.6 mol% acid copolymer. The spectra of the cation-exchanged forms include an arbitrary offset.

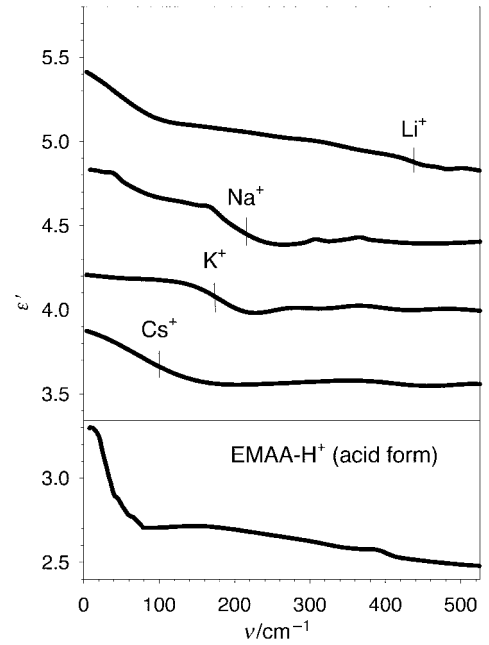

Fig. 5 Far-infrared ε' spectra of the H^+(acid), Cs^+, K^+, Na^+ and Li^+ forms of the EMAA copolymers. The K^+ form is that of the 5.4 mol% acid material and is shown 50% reduced in scale for ease of comparison with the other spectra, all of which are of the 2.6 mol% acid copolymer. The spectra of the cation-exchanged forms include an arbitrary offset.

Discussion

Analysis of the mid-infrared NISR spectra of PE(ox)

An early investigation[26] of oxidized low density polyethylene postulated the existence of various carbonyl functionalities based on a comparison of its spectrum with those of polyethylene in which model compounds had been dissolved. Whitesides and co-workers observed[27] a peak maximum at 1710 cm^{-1} in the ATR infrared spectra of their chromic acid-oxidized low

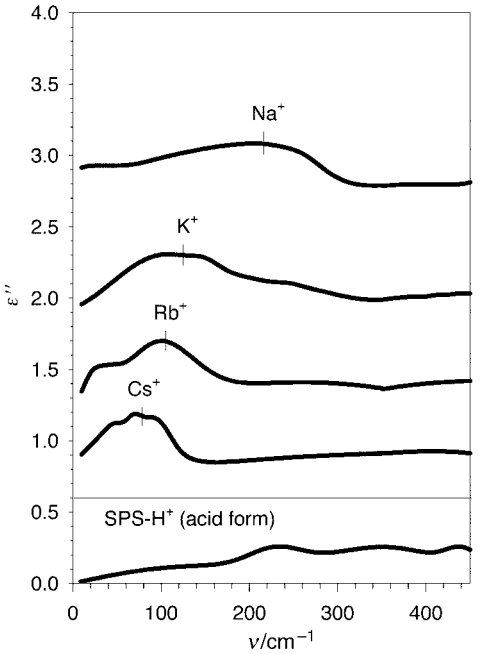

Fig. 6 Far-infrared ε'' spectra of the H^+ (acid), Cs^+, Rb^+, K^+ and Na^+ forms of the 12.8 mol% acid SPS materials. The spectra of the cation-exchanged forms include an arbitrary offset.

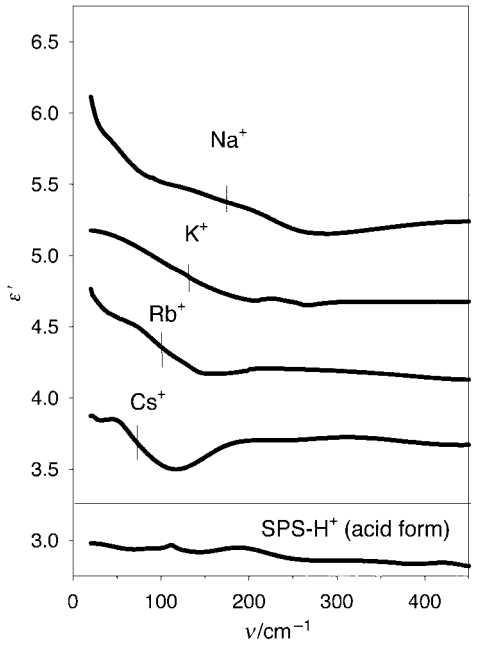

Fig. 7 Far-infrared ε' spectra of the H^+ (acid), Cs^+, Rb^+, K^+ and Na^+ forms of the 12.8 mol% acid SPS materials. The spectra of the cation-exchanged forms include an arbitrary offset.

density polyethylene and assigned it to the asymmetric C=O stretching vibration of the carboxylic acid dimer (associated, hydrogen bonded groups), whereas the corresponding band for the monomer (−COOH alone) is at 1750 cm^{-1}. The remaining spectral absorbances of samples that had been treated with base were assigned either to carboxylic acid groups that were unexchanged due to steric or pK_a constraints, or to ketone and aldehyde groups. They concluded that the chromic acid-oxidation process primarily resulted in the introduction of surface carboxylic acid groups and that only the dimer form of carboxylic acid is present.

Some differences between the results of this investigation, in which we find that both the monomeric form and dimeric

form of surface carboxylic groups are present on the surface of chromic acid-oxidized low density PE, and that of the earlier work,[27] in which only the dimeric form was present, are not unexpected. Even though identical chromic acid solution concentrations, oxidation temperatures and times were used, low density PE samples from different sources were used, and the polymers may differ in molecular mass and in such properties as crystallinity and surface morphology because of their different processing conditions. Furthermore, the surface was annealed prior to chromic acid oxidation in this work. However, it seems clear that both monomer and dimer acid groups are observed in this work.

Analysis of the far-infrared NISR spectra

The variation in ion-motion band positions with cation identity for the EMAA and SPS ionomers is in good agreement with previously reported results[5–8] obtained from transmission experiments. The same trend of decreasing frequency with increasing cation mass was observed. The ion-motion bands appear at somewhat higher frequencies in transmission than when measured by NISR. Differences between the results of the present and previous investigations of the EMAA- and SPS-based ionomers are not unexpected because the spectral quantities measured (ε'' *vs.* $\%T$), sample regions measured (bulk *vs.* near surface region), and thermal history of the samples are not the same. The nature of the band shapes of ion-motion bands was discussed previously in our investigations of ionomers[6] and glasses.[9,24]

The ion-motion band frequencies of the PE(ox-M^+) materials are somewhat lower than those of the EMAA-M^+ materials. Some differences between the ion-motion vibrations of the PE(ox-M^+) and analogous bulk ionomer materials are expected, because the oxidation treatment and the subsequently formed ion pairs are confined to the near surface region of the PE. Ion-pairs in bulk ionomers, in contrast, tend to form larger three-dimensional aggregates or clusters.[28] Ion-motion band frequencies in the bulk ionomers decrease with (1) increases in the cation–anion reduced mass, which is associated with increases in the cluster size, or (2) decreases in the force field element for this vibrational mode. The lower ion-motion band frequencies of the PE(ox-M^+) materials are postulated to be due to a lower force constant for the less constrained alkali ions at surface carboxylate sites.

Variation in $\Delta\varepsilon'$ with cation identity

The value of $\Delta\varepsilon'$ determined in this study for ionomers in the infrared, whether the far-infrared is considered alone or in conjunction with the mid-infrared, varies with cation in a manner similar to that of the alkali halide crystals.[29] That is $\Delta\varepsilon'$ falls in the order: $Li^+ > Na^+ > K^+ > Rb^+ > Cs^+$. This result is opposite to that for the electronic polarizability[29] of the cations themselves, which increases as $Li^+ < Na^+ < K^+ < Rb^+ < Cs^+$. This variation of $\Delta\varepsilon'$ with cation identity for the ionomers as well as alkali halides is best understood on the basis of dipole moment changes, $(\Delta\mu/\Delta q)_0$, contributing to the oscillator strength and thus magnitude of ε''. Since ε'' and ε' are not independent of each other (due to causality), the magnitude of $\Delta\varepsilon'$ about a resonance absorption tends to increase for absorbances with larger oscillator strengths (ε''). The dipole moment change associated with the vibrations of a light cation is greater than that of a heavier cation primarily because the extent of charge displacement during the vibration is greater, although differences in ionic character of the bond and effective charge on the ions can also affect the value of the oscillator strengths. Relaxation mechanisms associated with ion-motion bands or the far-infrared spectral region are discussed in our report[24] on glasses, in Salomon and co-workers' investigations[30] on alkali ion salts dissolved in solutions of polyethers, and Vij and Hufnagel's investigations[31] on aliphatic ketones. Several excellent reviews of dielectric relaxation in the infrared region[13,29] and in polymers[32] have been written.

Spectral results and adhesion calculations

Dispersion forces[13] between macrobodies are commonly calculated in Lifshitz theory[33] using quantum field theory to treat the macrobodies as continuous media. This assumes that the distances between the surfaces of the interacting bodies are small but significantly larger than the interatomic dimensions in the macrobodies. It allows their atomic structures to be ignored and makes it possible to calculate the forces from the dielectric properties, which are expressed by $\varepsilon^*(\omega)$, where $\varepsilon^*(\omega)=\varepsilon'(\omega)+i\varepsilon''(\omega)$.

The practical calculation of dispersion forces is done more readily with a real dielectric function evaluated along an imaginary frequency axis,[13–15,33] $\varepsilon(i\xi)$, in a complex frequency plane, ω^*, where $\omega^*=\omega'+i\xi$, than with the complex dielectric function, ε^*, evaluated along a real frequency axis, ω. A Kramers–Kronig transformation (KKT) was used in the present investigation to calculate[13] $\varepsilon(i\xi)$ directly from the $\varepsilon''(\omega)$ sample spectra in the manner of eqn. (1) between 4000 and 20 cm^{-1}.

$$\varepsilon(i\xi)-1=\left(\frac{2}{\pi}\right)\int_0^\infty \frac{\omega\varepsilon''(\omega)}{\omega^2+\xi^2}\,d\omega \qquad (1)$$

$\varepsilon(i\xi)$ could be calculated[13,15] instead based on the band parameters determined from a band-fitting analysis of the $\varepsilon''(\omega)$ sample spectrum. This alternative method introduces an additional level of complexity compared to the method used here and is, of course, quite dependent on the quality of the band-fitting analysis. The function $\varepsilon(i\xi)$ decreases monotonically from the static relative permittivity, ε_0 (*i.e.* when $\xi=0$) to a value of 1 when $\xi=\infty$. The function $\varepsilon(i\xi)$ resembles $\varepsilon'(\omega)$ since both functions can be obtained from a KKT of $\varepsilon''(\omega)$, and the latter also decreases when the frequency of the field increases. The function $\varepsilon(i\xi)$ contains all the information necessary for the calculation of the dispersion interaction.

Calculation of the non-retarded dispersion interaction between two bodies, which have dielectric permeabilities $\varepsilon_1(i\xi)$ and $\varepsilon_2(i\xi)$, involves calculating the average angular frequency,[13] $\bar{\omega}$, from the functions $\varepsilon_i(i\xi)$ for the two bodies($i=1,2$) as in eqn. (2).

$$\bar{\omega}=\int_0^\infty \left(\frac{\varepsilon_1(i\xi)-1}{\varepsilon_1(i\xi)+1}\right)\left(\frac{\varepsilon_2(i\xi)-1}{\varepsilon_2(i\xi)+1}\right)d\xi \qquad (2)$$

The dispersion force between two bodies can be calculated[13] from this averaged angular frequency in a manner consistent with the geometry of the system. For two infinite planes in contact with each other this can be done as in eqn. (3).

$$F^{LW}=\frac{\hbar\bar{\omega}}{8\pi^2 Z^3} \qquad (3)$$

The Hamaker constant, A_H, which is essentially a measure of the free energy of the interaction between two bodies, has contributions from all three electrodynamic interactions in condensed bodies (dispersion, orientation and induction). However, in polar condensed media the only significant contribution usually comes from the dispersion interaction. The Hamaker constant can be then calculated[13] as in eqn. (4).

$$A_H=\frac{3\hbar\bar{\omega}}{4\pi} \qquad (4)$$

The relative importance of contributions to $\bar{\omega}$ from various spectral regions has been the subject of considerable debate.[13,34–37] Frequencies having larger values of $\varepsilon'(\omega)$, and thus $\varepsilon(i\xi)$, would be expected to make larger contributions to $\bar{\omega}$. Both of these functions increase with decreasing frequency

as they approach the static value, ε_0, and that tends to favor the contribution of lower frequency regions such as the infrared and far-infrared measured in this study. On the other hand, the visible and UV regions span a much greater frequency range, so their contribution is often taken to be more important.

An important consideration in evaluating the importance of various spectral regions is that the contributions of the dielectric properties in the various spectral regions depend on distance. The non-retarded interaction [eqn. (2)] applies when the surfaces of the two bodies are in intimate contact so that the distance of separation between the surfaces is much smaller than the wavelength of electromagnetic radiation under consideration. Then the interaction between oscillators in the two bodies is essentially instantaneous with no loss of phase coherence.[13] This condition is met for wavelengths, λ, greater than some wavelength, λ_0. The propagation time is given by Z/c, where Z, the separation distance, must be much less than the characteristic time for the internal motion, or the period for the harmonic oscillator, ($\approx 2\pi/\omega_0$), such that eqn. (5) holds.

$$Z \ll 2\pi c/\omega_0 = \lambda_0 \quad (5)$$

Thus the retarded interaction favors the contribution of longer wavelength electromagnetic radiation to the dispersion interaction as the distance of separation, Z, increases between two bodies and the contribution of shorter wavelength electromagnetic radiation is damped out.

The $\varepsilon(i\xi)$ spectra of the polymers and of a flat Pyrex glass substrate were calculated from their respective $\varepsilon''(\omega)$ spectra shown in Fig. 2–5 and described in Tables 1 and 2. The values of $\bar{\omega}$, A_H, and F^{LW} for the dispersive interaction due to polarization mechanisms at infrared frequencies of EMAA copolymers and the PE(ox) materials with the glass substrate were computed from the respective $\varepsilon(i\xi)$ spectra and are in Table 3.

The $\bar{\omega}$ values, Hamaker constants and adhesion forces are observed to vary for the 2.6 mol% acid EMAA copolymers as: EMAA-H^+ > EMAA-Li^+ > EMAA-Na^+ > EMAA-Cs^+. The 5.6 mol% H^+-EMAA has a greater $\bar{\omega}$ value than the 2.6 mol% acid H^+-EMAA copolymer, although the variation in $\bar{\omega}$ with acid group content is smaller than the variation in $\Delta\varepsilon'$. In Table 3, the $\bar{\omega}$, A_H, and F^{LW} values for the interaction at far-infrared frequencies of low density PE(ox) materials (both H^+ and M^+ forms) with a Pyrex glass substrate are included. The $\bar{\omega}$, A_H and F_{LW} values vary with cation identity in a manner similar to that of the EMAA copolymers, which are also shown in Table 3, although the variation is somewhat smaller in the case of the PE(ox) materials.

Our calculated $\bar{\omega}$ values, Hamaker constants and dispersion forces for the EMAA ionomers vary with cation identity in a manner that is qualitatively consistent with the reported adhesion strengths of Lipatov[19] for the adhesion of polyurethane ionomers to various substrates and with the T peel strengths for these polymers bound to a polymer composite substrate, reported by Brack.[20]

Since the $\bar{\omega}$ values increase with the acid content of the EMAA copolymer, as well as with the identity of the cation, the variation in $\bar{\omega}$ values and dispersion forces with cation identity is expected to increase with the extent of exchange of alkali cations for protons. Infrared analysis showed that the extent of exchange for our metal–EMAA materials was about 60% exchange. Thus, the variation in the calculated $\bar{\omega}$ values with cation identity reported here is probably less than would be seen if the material were 100% exchanged.

Our calculated $\bar{\omega}$ values, Hamaker constants and dispersion forces for PE(ox) also vary with cation identity in a manner consistent with the calculated values for the EMAA copolymers and with the reported peel strengths[20] for the EMAA copolymers, although their variation with cation identity is somewhat less than that calculated for the EMAA copolymers. This difference is not that surprising in that the penetration depth of the IR beam during the specular reflectance measurement is greater than the functionalization depth during the chromic acid etching. There is therefore a higher concentration of carboxylic acid and ionic groups in the total surface region (greater number of oscillators) probed by the infrared NISR experiment for the EMAA copolymers, where they are distributed throughout the depth of the material, than for PE(ox), where they are restricted to the near surface. Another important reason for the greater calculated forces for EMAA *versus* PE(ox) is that a greater spectral region (mid- and far-IR regions) was used in the calculations of F^{LW} for EMAA *versus* PE(ox) (only the far-IR).

There is little reported quantitative adhesion data with which to compare our calculated $\bar{\omega}$ and F^{LW} values. However, Briggs and Kendall[38] have reported that the measured peel strengths of NaOH exchanged PE(ox) materials were significantly less than those measured for the unexchanged PE(ox) materials. This is in agreement with our calculated results.

In comparing calculated forces with experimentally determined ones, it is important to note that not all frequencies have been included in these calculations of $\bar{\omega}$, so the calculated dispersion forces are smaller than would be obtained if the contributions of all frequencies had been included. It is also important to note that the dispersion force is only one of several contributions to adhesion, and that significant contributions to the adhesion of the systems could then come from other mechanisms such as hydrogen bonding. This is likely to be an important factor in the adhesion of ionomers to various substrates both as carboxylic acid donors in the unexchanged EMAA copolymers and as carboxylic acid donors and carboxylate acceptors in the incompletely exchanged EMAA copolymers.

Table 3 Calculated $h\bar{\omega}$, A_H and F^{LW} for the interaction of EMAA copolymers and PE(ox) with plate glass

polymer	mol% acid	exchanged cation	$h\bar{\omega}$/eV	A_H/eV	F^{LW}/eV Å^{-3}[a]
EMAA	2.6	$-(H^+)$	2.54×10^{-2}	6.07×10^{-3}	1.19×10^{-8}
EMAA	2.6	Li^+	2.46×10^{-2}	5.88×10^{-3}	1.15×10^{-8}
EMAA	2.6	Na^+	2.34×10^{-2}	5.59×10^{-3}	1.09×10^{-8}
EMAA	2.6	Cs^+	2.22×10^{-2}	5.30×10^{-3}	1.04×10^{-8}
EMAA	5.4	H^+	2.68×10^{-2}	6.40×10^{-3}	1.25×10^{-8}
EMAA	5.4	K^+	2.49×10^{-2}	5.95×10^{-3}	1.16×10^{-8}
PE(ox)	—	$-(H^+)$	3.43×10^{-3}	8.20×10^{-4}	1.60×10^{-9}
PE(ox)	—	Li^+	3.37×10^{-3}	8.05×10^{-4}	1.58×10^{-9}
PE(ox)	—	Na^+	3.35×10^{-3}	8.01×10^{-4}	1.57×10^{-9}
PE(ox)	—	K^+	3.31×10^{-3}	7.91×10^{-4}	1.55×10^{-9}
PE(ox)	—	Rb^+	3.29×10^{-3}	7.86×10^{-4}	1.54×10^{-9}
PE(ox)	—	Cs^+	3.27×10^{-3}	7.82×10^{-4}	1.53×10^{-9}

[a]For 30 Å separation.

Conclusions

The change in polarizability, as determined by $\Delta\varepsilon'$, in the mid- and far-infrared regions was found to vary with ionic content and cation identity for the ionomers and PE(ox). $\Delta\varepsilon'$ was found to increase with increasing ionic content and to vary as PE(ox-Li^+) > PE(ox-Na^+) > PE(ox-K^+) > PE(ox-Rb^+) > PE(ox-Cs^+) for surface oxidized polyethylene, as SPS-Li^+ > SPS-Na^+ > SPS-K^+ > SPS-Rb^+ > SPS-Cs^+ > SPS-H^+ > PS for the SPS and PS polymers, and as EMAA-H^+ > EMAA-Li^+ > EMAA-Na^+ > EMAA-K^+ > EMAA-Cs^+ for the EMAA copolymers. The calculated dispersion forces for the interaction of these materials with a Pyrex glass substrate due to the motions in far- and mid-infrared regions were found to vary in an identical manner as $\Delta\varepsilon'$ for the EMAA copolymers and PE(ox) materials, which is consistent with reported adhesion

strength measurements of other ionomers with various substrates.[19–20] However, the variation was of greater magnitude in the experimentally measured adhesion strengths[19–20] than was calculated here for the mid- and far-infrared contribution to the dispersion force.

We wish to thank M. Doll of Brown University for assistance with computer programming. H.P.B. gratefully acknowledges the financial support of Brown University and the US Department of Education in the form of Brown University and GAANN fellowships.

References

1 J. N. Israelachvili, *Intermolecular and Surface Forces,* 2nd edn., Academic, New York, 1991.
2 W. F. Edgell, A. T. Watts, J. Lyford and W. M. Risen Jr., *J. Am. Chem. Soc*., 1966, **88**, 1815.
3 B. W. Maxey and A. I. Popov, *J. Am. Chem. Soc*., 1967, **89**, 2230.
4 G. B. Rouse, W. M. Risen Jr., A. T. Tsatsas and A. Eisenberg, *J. Polym. Sci., Polym. Phys. Ed*., 1979, **17**, 81.
5 A. T. Tsatsas and W. M. Risen, *Chem. Phys. Lett*., 1970, **7**, 354.
6 A. T. Tsatsas, J. W. Reed and W. M. Risen Jr., *J. Chem. Phys*., 1971, **55**, 3260.
7 V. D. Mattera and W. M. Risen Jr., *J. Polym. Sci., Polym. Phys. Ed*. 1984, **22**, 67.
8 V. D. Mattera, S. L. Peluso, A. T. Tsatsas and W. M. Risen Jr., in *Coulombic Interactions in Macromolecular Systems,* ed. A. Eisenberg and F. E. Bailey, ACS Symp. Ser. 302, ACS, Washington DC, 1984, p. 54.
9 G. J. Exarhos, P. J. Miller and W. M. Risen Jr., *J. Phys. Chem.,* 1974, **60**, 4145.
10 A. T. Tsatsas, R. W. Stearns and W. M. Risen Jr., *J. Am. Chem. Soc*., 1972, **94**, 5247.
11 D. P. Cobranchi, B. A. Garland, M. C. Masiker, E. M. Eyring, P. Firman and S. Petrucci, *J. Phys. Chem*., 1992, **96**, 5856.
12 W. M. Butter, C. C. Angell, W. A. McAllister and W. M. Risen Jr., *J. Phys. Chem*., 1977, **81**, 2061.
13 J. Mahanty and B. W. Ninham, *Dispersion Forces*, Academic, New York, 1976, ch. 2.
14 D. Gingell and V. A. Parsegian, *J. Theor. Biol*., 1972, **36**, 41.
15 V. A. Belyi, V. A. Smurugov and A. I. Sviridyonok, in *Adhesion and Adsoption of Polymers,* Polymer Science and Technology Vol. 12A, ed. L. H. Lee, Plenum, New York, 1979, p. 67.
16 D. C. Prieve and W. B. Russel, *J. Coll. Int. Sci*., 1988, **125**(1), 1.
17 J. Visser, in *Surface and Colloid Science*, ed. E. Matijevic, Wiley-Interscience, New York, 1976, vol 8; ch. 1.
18 Y. A. Rabinovich and N. V. Churaev, *Coll. J. USSR,* 1984, **46**(2), 290.
19 Y. S. Lipatov, L. M. Sergeeva, E. Y. Gorichko and A. A. Brovko, *Vysokomol. Soedin., Ser. B*, 1984, **26**(9), 643; Chem. Abstr. 102: 47376s.
20 H. P. Brack, PhD Thesis, Brown University, May 1994.
21 J. S. Tan, in *Structure and Properties of Ionomers,* ed. M. Pineri and A. Eisenberg, NATO ASI Ser. C: Math. Phys. Sci., Reidel, Dordecht, Holland, 1987, vol. 198 p. 429.
22 D. K. Jenkins and E. W. Duck, in *Ionic Polymers,* ed. L. Holliday, Wiley, New York, 1975, ch. 3.
23 H. P. Brack and W. M. Risen Jr., *Polymer Preprints,* 1991, **32**(3), 653.
24 A. Burns, H. P. Brack and W. M. Risen Jr., *J. Non-Cryst. Solids*, 1991, **131–133,** 994.
25 W. J. MacKnight, L. W. McKenna, B. E. Read and R. S. Stein, *J. Phys. Chem*., 1968, **72**(4), 1122.
26 F. M. Rugg, J. J. Smith and R. C. Bacon, *J. Polym. Sci*., 1954, **13**, 535.
27 J. R. Rasmussen, E. R. Stedronsky and G. M. Whitesides, *J. Am. Chem. Soc*., 1977, **99**(14), 4736.
28 A. Eisenberg, B. Hird and R. B. Moore, *Macromolecules*, 1990, **23**(18), 4098.
29 I. Bunget and M. Popescu, *Physics of Solid Dielectrics,* Mater. Sci. Monographs 19, Elsevier, New York, 1984, ch. 6.
30 M. Salomon, M. Xu, E. M. Eyring and S. Petrucci, *J. Phys. Chem*., 1994, **98**, 8234.
31 J. K. Vij and F. Hufnagel, *J. Phys. Chem*., 1991, **95**, 6142.
32 S. Havriliak Jr. and S. J. Havriliak, *Dielectric and Mechanical Relaxation in Materials: Analysis, Interpretation and Application to Polymers,* Hanser, Munich, 1997.
33 I. E. Dzyaloshinski, E. M. Lifshitz and L. P. Pitaevski, *Adv. Phys.,* 1961, **10**, 165.
34 J. Visser, *Adv. Coll. Int. Sci*., 1972, **3**, 331.
35 B. W. Ninham and V. A. Parsegian, *J. Chem. Phys*., 1970, **52**(9), 4578.
36 S. Nir, R. Rein and L. Weiss, *J. Theor. Biol*., 1972, **34**, 135.
37 H. Krupp, *Adv. Coll. Int. Sci*., 1967, **1**, 111.
38 D. Briggs and C. R. Kendall, *Int. J. Adhesion and Adhesives*, 1982, **2**, 13.

Paper 7/02686B; *Received* 21*st April*, 1997